3. Atomic Resonance and Scattering

Academic and Research Staff

Prof. D. Kleppner, Prof. D.E. Pritchard, Dr. R. Ahmad-Bitar, Dr. T. Ducas, Dr. D. Kelleher, Dr. M. Ligare, Dr. A.M. Lyyra, Dr. P. Moskowitz, Dr. K.L. Saenger, Dr. N. Smith, Dr. W.P. Spencer, Dr. G. Vaidyanathan, Dr. X. Zhong

Graduate Students

S. Atlas, V. Bagnato, L. Brewer, S.L. Dexheimer, R. Flanagan, T.R. Gentile, P.L. Gould, E. Hilfer, B.J. Hughey, R.G. Hulet, M.M. Kash, P.D. Magill, A.L. Migdall, W.P. Moskowitz, E. Raab, T.P. Scott, B.A. Stewart, R. Weisskoff, G.R. Welch

Undergraduate Students

I. Nir, K. Plonty, D. Sherman

3.1 Rydberg Atoms in a Magnetic Field

National Science Foundation (Grant PHY79-09743)

Michael M. Kash, Daniel Kleppner, Ishai Nir, George R. Welch

The general structure of atomic hydrogen in an arbitrarily strong magnetic field is still an unsolved problem of atomic physics. The diamagnetic Hamiltonian for hydrogen is known; the eigenstates are not. Highly excited, or Rydberg, atoms in a laboratory sized field (about 10 Tesla) exhibit strong principal quantum number "mixing". Even numerical solutions fail in this regime.

The experimental goal of our research is to map out the energy levels of a Rydberg lithium atom in a strong magnetic field in the vicinity of a crossing between levels from different principal quantum numbers. The scheme for producing the Rydberg atoms by optical excitation with lasers is 2s→3s via two photons (735 nm) and 3s→~40p via one photon (~620 nm). The atoms are detected by field ionization.

We have observed the two-photon transition by monitoring the cascade fluorescence to the ground state. Fig. 3-1 shows the two-photon transition in ^{7}Li, and Fig 3-2 shows the two-photon transition in ^{6}Li. The measurements are in an atomic beam of "natural" lithium in which only 7% is ^{6}Li. The markers are 300 MHz. Using the accurately known ground state hyperfine structure intervals, we have obtained the $3^2S_{1/2}$ hyperfine structure intervals: 190(20) MHz for ^{7}Li, and 50(20) MHz for ^{6}Li.

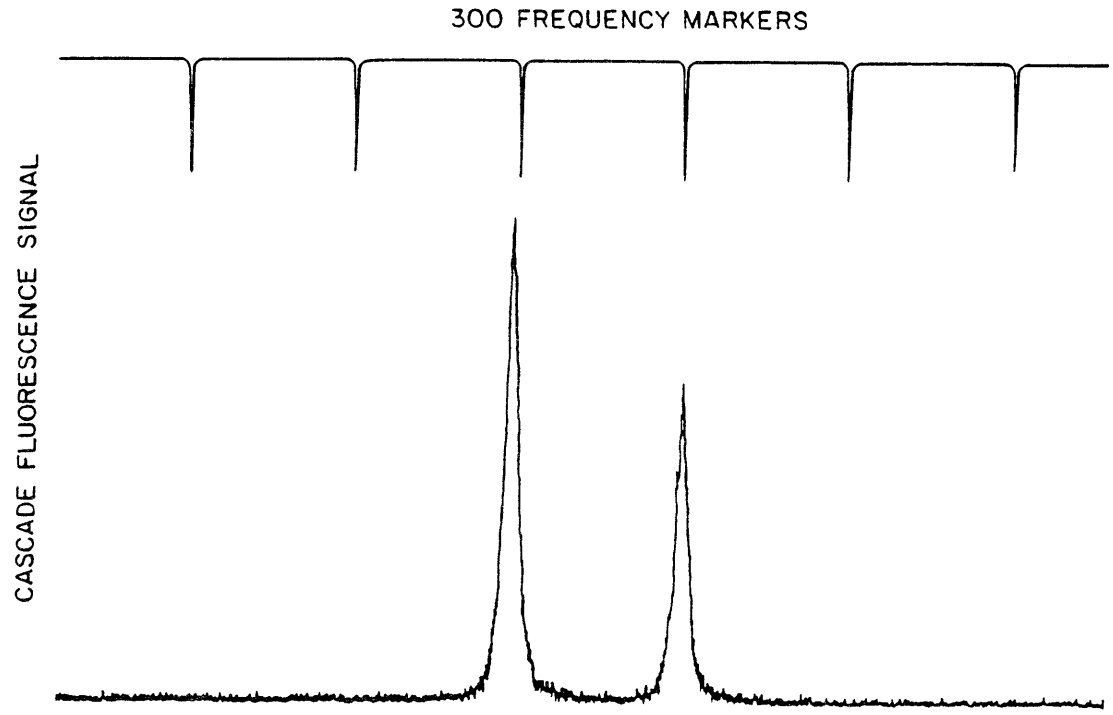

Figure 3-1: Two-Photon Absorption from 2s→3s in ^{7}Li

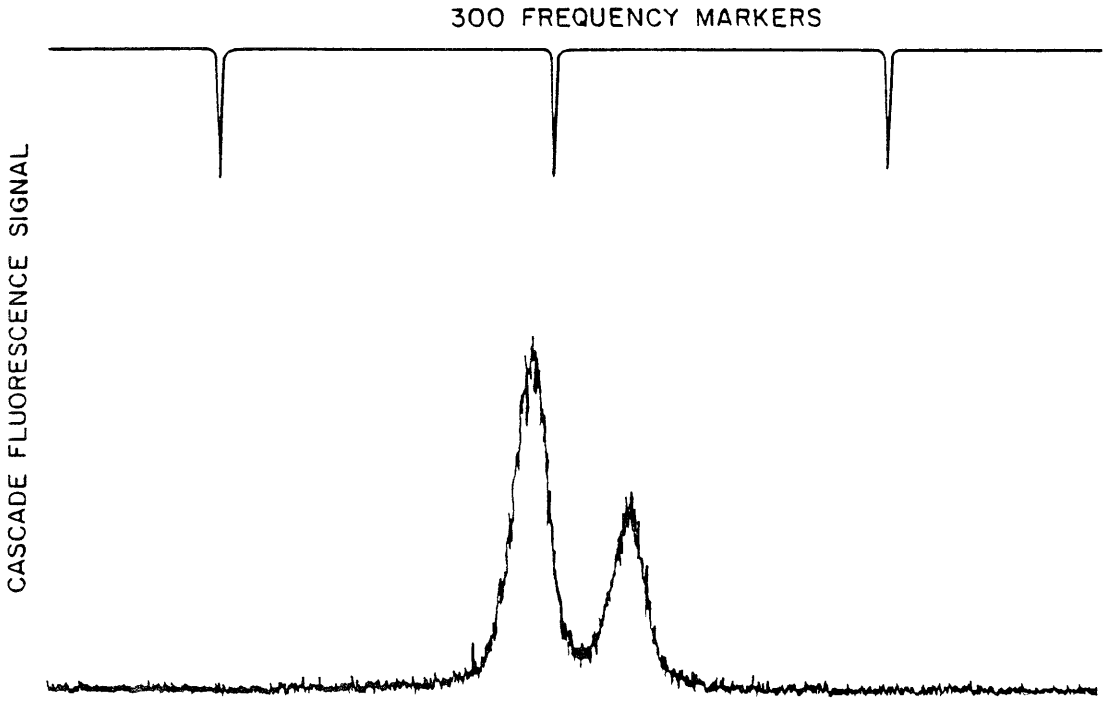

Figure 3-2: Two-Photon Absorption from 2s→3s in ^{6}Li

3.2 Electrodynamics in a Cavity

National Science Foundation (Grant PHY82-10486)
Joint Services Electronics Program (Contract DAAG29-83-K-0003)
U.S. Navy - Office of Naval Research (Contract N00014-79-C-0183)
Thomas R. Gentile, Barbara J. Hughey, Randall G. Hulet, Daniel Kleppner, William P. Spencer, A. Ganesh Vaidyanathan

Spontaneous emission of a photon by an excited atom depends on the nature of the space surrounding the atom. In free space, the photon can be emitted into the infinite number of modes of the radiation field which can support the photon. In a cavity, the number of modes is restricted, and this radically alters the way the atom emits radiation. With the cavity off resonance, spontaneous emission is inhibited. On resonance, the atom–cavity system oscillates between an excited atom with no photon, and a de–excited atom with a photon.

We are investigating these phenomena with our experiments on the electrodynamics of Rydberg atoms in a cavity. We also hope to study enhanced spontaneous emission, "super cooling" of the radiation field, and to observe the statistical behavior of small numbers of atoms interacting with small numbers of photons. In our initial experiments, we have observed a related phenomenon, enhanced absorption of blackbody radiation (see Fig. 3–3). These experiments enhance our understanding of atom–photon interactions at the single photon–single atom level as well as increasing our understanding of fundamental noise processes. The experimental methods have applications in the development of ultra sensitive far–infrared detectors.

The experiments are carried out in an atomic beam of sodium. The atoms are excited to a Rydberg state by pulsed dye lasers and then pass through a high Q ($\sim 10^7$) superconducting cavity. As the atoms leave the cavity, they are analyzed in a special detector which determines not only their final state but the time spent in the cavity. Much of the work over the past year has been devoted to perfecting the novel state selective detector and in developing the tunable super conducting cavity.

The Rydberg atom detector uses an inhomogeneous electric field to spatially resolve the state of the Rydberg atom (see Fig. 3–4). This has four advantages over the more commonly used time resolved pulsed field ionization: 1) Rydberg atoms can be individually counted; 2) The velocity of the Rydberg atoms can be directly measured; 3) All Rydberg atoms are collected; and 4) The detector may be used for detection of a continuous beam of Rydberg atoms.

A super conducting cavity with a Q of about 10^6 has been constructed. We are currently working to improve the Q cavity to 10^7, and to install a mechanism to tune the cavity. At 30 GHz, a cavity with a Q of 10^7 needs a tuning resolution of at least 1 kHz. Tuning is achieved by "squeezing" the cavity. We are using the TM_{010} mode of the cavity, which allows the cavity cylinder to be cut along its axis of symmetry. "Squeezing" is achieved by separating the two halves slightly and moving them together.

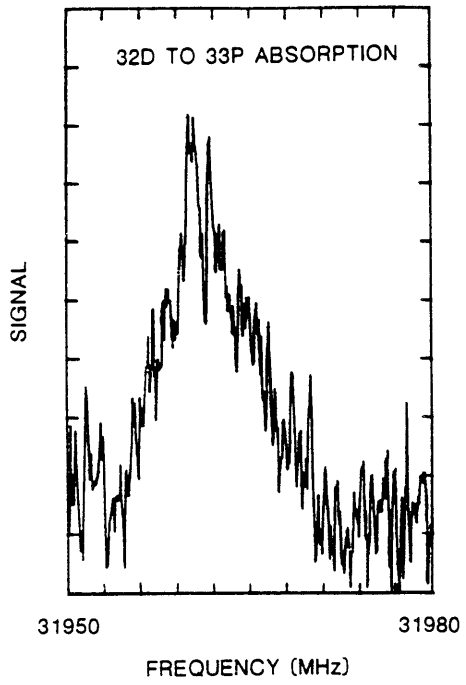

Figure 3-3: Enhanced absorption of blackbody radiation. Rydberg atoms are placed on the 32d state of sodium inside of a 77 K cavity. As the cavity is tuned on resonance, transfer of population from the 32d to the 33p state is observed. The transfer rate is increased on resonance by a factor of 10^4, the Q of the cavity. Total transfer is limited by collective atom effects inside the cavity.[2]

A motion of 10^{-7} cm corresponds to 1 KHz.

We are also working to observe inhibited spontaneous emission, using our recently developed techniques of populating Rydberg atoms in "circular" states.[1] These are Rydberg states with highest angular and orbital momentum. Because of selection rules, only one channel of spontaneous decay is available. If we place these atoms in a cavity beyond cutoff, no spontaneous emission can occur. The Rydberg state effectively becomes a new ground state for the atom.

References

1. R. Hulet and D. Kleppner, Phys. Rev. Lett. 51, 1430 (1983).
2. J.M. Raimond, P. Goy, M. Gross, C. Fabre, and S. Haroche, Phys. Rev. Lett. 49, 117 (1982).

3.3 Multiphoton Ionization

National Science Foundation (Grant PHY79-09743)
National Bureau of Standards (Grant NB83-NAHA-4058)
Lawrence Brewer, Daniel Kellcher, Daniel Kleppner, Martin Ligare

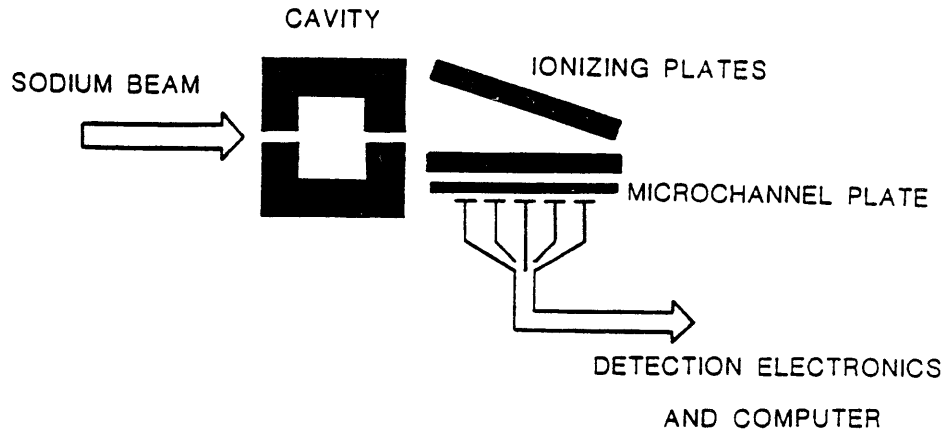

Figure 3-4: A novel detection scheme is employed for determining the final state of the Rydberg atom. A set of field plates are tipped with respect to one another by 5°. As the atom drifts into the detection region it experiences an increasing field until it ionizes. The position and time of the resulting electron is recorded by an array of collector strips. The position determines the final states of the atom and the time determines the velocity of the atom.

Multiphoton ionization of atoms and molecules is a non-linear phenomenon which can occur whenever matter interacts with intense optical fields such as those produced by high power lasers. Of particular interest to us is resonance enhanced multiphoton ionization. This occurs when the photon energy matches an allowed intermediate transition in the multiphoton absorption process. The multiphoton resonance absorption profile is affected by the shifts and ionization broadening of the intermediate energy levels due to the intense fields used to observe multi-photon ionization. Because multiphoton ionization is a non-linear process, the rate is sensitive to amplitude and phase fluctuations of the field. We have studied these processes in the four-photon ionization of atomic hydrogen. Three photon excitation is resonant with the 1s-2p transition of the atom, and the fourth photon ionizes the atom at threshold.

The experiment is carried out in a cooled atomic beam. Atomic hydrogen is generated from molecular hydrogen in an rf dissociator and then passed through an accomodator which can be cooled to liquid nitrogen or helium temperature. The multiphoton ionization requires photons near 364.6 nm. We use the frequency doubled output of a Nd:YAG laser to pump a dye laser-amplifier combination which produces tunable output near 554.6 nm. This is mixed in a non-linear crystal with the fundamental frequency of the ND:YAG laser at 1064 nm to give tunable light near 364.6 nm. This

produces 10 mJ pulses of 9 nsed duration. The photoions created by the laser pulse are swept out of the interaction region by a pair of field plates and are collected in an electron multiplier.

Fig. 3–5 shows a typical experimental lineshape for a 4.5 mJ pulse (about 15 GW/cm^2). The line profile is highly asymmetric, shifted to the blue from the zero field 1s–2p resonance, and very broad. As the laser power is increased the shift and width increase approximately linearly. The height of the peak of the profile grows with the third power of the laser intensity. Theory for a perfectly monochromatic light field indicates that the lineshape should be Lorentzian with a shift governed by the "A.C." Stark shift and with a width given by the ionization rate of the 2p state. The peak of the resonance profile should grow as the square of the laser intensity.[1]

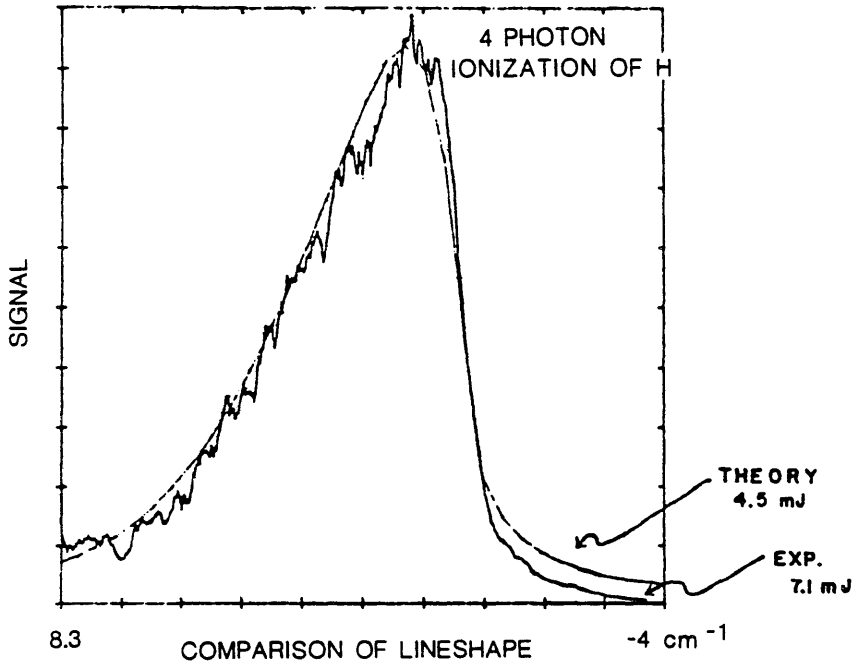

Figure 3-5: Comparison of the shape of experimental and theoretical resonance profiles for four photon multiphoton ionization of atomic hydrogen. Note that the power density used to generate the theoretical profile is not the same as the power density used for the experimental profile.

The experimentally observed effects can be understood qualitatively by averaging the Lorentzian lineshape (which is predicted for a constant amplitude monochromatic field) over the distribution of field amplitudes that occur in our finite bandwidth, multimode laser pulses. In addition, the theoretical results must be averaged over the spatial intensity distribution of a gaussian laser beam. This averaging yields profiles like that designated 'theory' in Fig. 3–5. The long "blue tail" of the profile is the result of contributions from the high intensity peak amplitudes produced by the mode beating in the pulse. It is these high intensities which are responsible for large A.C. Stark shifts and ionization

widths. The shape of the profile is well reproduced, but the power density predicted by the theory for a particular value of the shift and width is lower than that given by the experiment. In addition, the power dependence of the height of the peak is not correctly accounted for in such a simple theory.

We are currently constructing a single mode tunable dye laser system. The amplitude and phase fluctuations of this light should be much reduced compared to our present system. We are also working on a more complete theory in an attempt to understand all the features of the experimental profiles.

References

1. C.R. Holt, M.G. Raymer, and W.P. Reinhardt, Phys. Rev. A 27, 2791 (1983).

3.4 Velocity Dependence of Rotational Rainbow Structure in $Na_2 - Ar$

National Science Foundation (Grant CHE79-02967-A04)

Warren P. Moskowitz, Brian A. Stewart, J.L. Kinsey, David E. Pritchard

We have measured level-to-level differential cross sections for the rotationally inelastic process $Na_2(j_i = 7) + Ar \rightarrow Na_2(j_f = j_i + \Delta J) + Ar$ at center of mass energies 0.49 and 1.1 eV, with Na_2 in its lowest electronic and vibrational state. The angular momentum transfer Δj ranged from 2 to 40. The measurements were made in crossed molecular beams. The initial rotational level was selected using optical pumping, and the final rotational level was detected by laser induced fluorescence. The angular distribution was determined by a new Doppler technique, called PADDS, that gives good small angle resolution. In this technique, a single mode, c.w. dye laser beam intersects the collision region perpendicular to the relative velocity vector, and excites molecules which have been scattered into the final state with the correct Doppler—selected velocity component in the direction of the laser. The laser is tuned, and the resulting fluorescence signal yields the differential cross section through a deconvolution. A typical differential cross section is shown in Fig. 3-6.

3.5 High Precision Mass Measurement on Single Ions Using Cyclotron Resonance

National Science Foundation (Grant PHY83-07172)

Riyad Ahmad-Bitar, Robert W. Flanagan, Phillip L. Gould, David E. Pritchard, Robert M. Weisskoff

In the past few years powerful new techniques for study of resonances in trapped particles have been developed.[1,2] We plan to apply these techniques to precision mass measurement of single atomic and molecular ions using a novel, low-noise detection scheme. These measurements permit advances in mass and x-ray wavelength metrology, chemistry, and physics. Measurement of relative

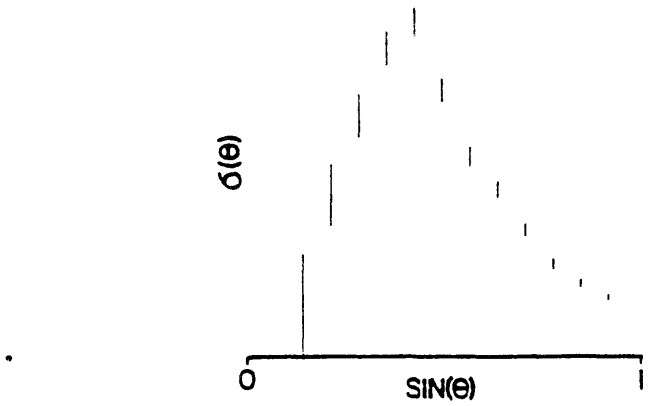

Figure 3-6: Differential cross section for $\Delta j = 16$, obtained by procedure described in paper submitted to J. Chem. Phys.

mass differences of one part in 10^{11} will permit the weighing of chemical bonds, ultra-precise measurement of energy differences in isomer nuclei, and improved knowledge of physical constants.

The experiments will involve capturing a single ion in a Penning trap and measuring the weak signals emitted as the ion oscillates. The small signals expected and the requirement for high precision demand the use of a SQUID (superconducting quantum interference device) detector, liquid helium-cooled coupling networks, and a high stability superconducting magnet. Single ion techniques are necessary since Van Dyck[2] has shown that space charge effects cause the cyclotron resonance to shift by about 1.2×10^{-10} per ion, even when using a compensated trap.

Currently, the cryogenic container, vacuum system and Penning trap are being designed. Modifications to commercial NMR magnet systems are being developed with assistance provided by several manufacturers. Some computer hardware has been purchased and some software has been developed. A stable voltage source (drift $\lesssim 10^{-8}$ per minute) has been constructed and our preliminary experiments with superconducting impedance matching circuits have been promising.

References

1. Robert S. Van Dyck, Jr., Paul B. Schwinberg, and Hans G. Dehmelt, in Daniel Kleppner and Francis Pipkin, (Eds.), Atomic Physics, Vol. 7 (Plenum Press, 1981) p. 340.
2. R.S. Van Dyck, Jr., and P.B. Schwinberg, Phys. Rev. Lett. 47, 395 (1981).

3.6 Intensity and Frequency Dependence of Atomic Beam Deflection by Transverse Standing Wave Radiation

National Science Foundation (Grant PHY83-07172)

Phillip E. Moskowitz, Phillip L. Gould, Susan Atlas, Eric Raab, David E. Pritchard

The deflection of an atomic beam by a standing wave laser field is a useful probe of the interaction of atoms with very intense optical radiation fields. We have studied this deflection as a function of laser intensity[1] and frequency by crossing a supersonic beam of sodium atoms with a perpendicularly oriented standing wave laser. The atomic beam is well collimated (4×10^{-5} rad) and has a narrow velocity distribution (10% FWHM). Total resolution of the apparatus is on the order of the momentum of a single photon ($p\gamma = hk$). The laser is tuned near the frequency of the $3S_{1/2} \rightarrow 3P_{3/2}$ transition and the interaction time is constrained to approximately one radiative lifetime (16 ns) in order to reduce the effects of spontaneous decay on the interactions.

Our results for the rms deflection as a function of laser power and frequency are shown in Figs. 3–7 and 3–8, respectively. The data are in rough agreement with semiclassical[2] and fully quantum mechanical[3] theories. Exact analysis is impossible due to the presence of multiple energy levels (hyperfine structure) in the sodium atom. However, the linear dependence of the deflection on electric field is evident at high fields and the frequency dependence is seen to have the predicted power-broadened resonance width.

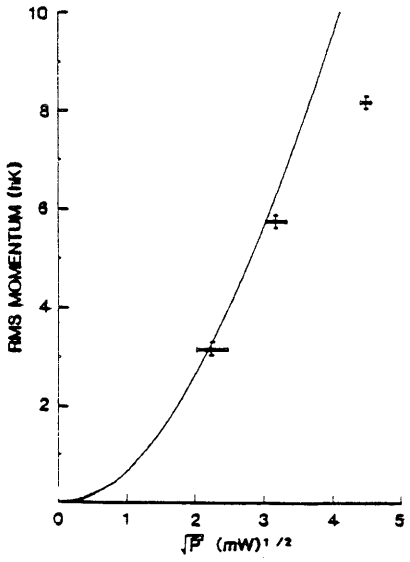

Figure 3-7:

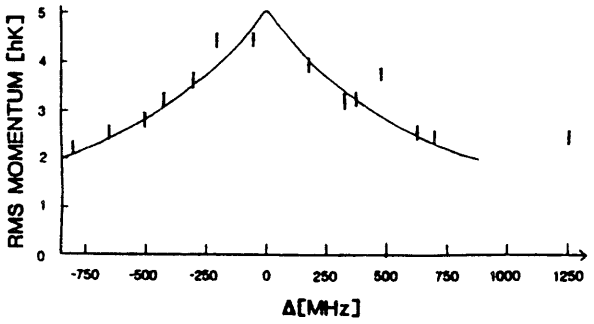

Figure 3-8:

References

1. P.E. Moskowitz, P.L. Gould, S. Atlas, and D.E. Pritchard, Phys. Rev. Lett. 61, 370 (1983).
2. A.P. Kazantsev, G.I. Surdutovich, and V.P. Yakovlev, JETP Lett. 31, 509 (1980).
3. A.F. Bernhardt and B.W. Shore, Phys. Rev. A 23, 1290 (1981).

3.7 Low Temperature Energy Transfer

Joint Services Electronics Program (Grant DAAG29-83-K-0003)
Alan L. Migdall, David E. Pritchard

We are investigating energy transfer collision processes at extremely low temperatures. Low temperatures were produced using a seeded supersonic beam source in which we have studied rotationally inelastic collisions for Li_2 – Ar at temperatures of 100°K and 250°K. Cross sections for these collisions were calculated from the data after accounting for the details of the expansion process. We are in the process of implementing a more accurate procedure to correct for the effects of multiple collisions.

We have fit our data to the ECS–EP law that has been used successfully on most of the existing rotationally inelastic data. We see some systematic deviation between our data and the fits, and we are testing to see if this deviation originates in our analysis or is an actual failure of the ECS theory.

We plan to make measurements using Li_2 – He. This system should dramatically show the effects of dynamical constraints due to the low mass of the collision partner, and hence the small amount of orbital angular momentum available to change j.

3.8 Trapping of Neutral Atoms

Vanderlei Bagnato, Riyad Ahman-Bitar, Phillip E. Moskowitz, David E. Pritchard, Eric Raab

Trapped atoms cooled below 10^{-7}K are an excellent system for studying collective phenomena (superradiance, Bose condensation, and phase transitions), studying collisions such as Na–Na or Na–Na*, and performing ultra–high resolution spectroscopy[1] with the possible objective of making a greatly improved frequency standard. Deceleration of a neutral atomic beam has been demonstrated recently by Phillips and Metcalf.[2,3] The next step is to trap the neutrals in a laboratory field and then cool them. Numerous schemes for such traps have been proposed including magnetic field traps,[1,4-7] electrostatic traps[8] and traps using near resonance radiation.[9,10] We have proposed schemes to cool the neutrals to 10^{-7}K in a magnetic field trap.

We are setting up an experimental apparatus to be used for decelerating and trapping atoms. Very briefly, the deceleration part is very much like Phillips et al.[3] The trapping of paramagnetic particles occurs in magnetic sublevels whose energy increases in proportion to the applied field. We are building such a trap whose well is 30 mK deep to trap the decelerated Na–beam.

References

1. D.E. Pritchard, Phys. Rev. Lett. 51, 1336 (1983).
2. W.D. Phillips and H. Metcalf, Phys. Rev. Lett. 48, 596 (1982).

3. J.V. Prodan, W.D. Phillips, and H.J. Metcalf, Phys. Rev. Lett. 49, 1149 (1982).
4. H. Friedberg and W. Paul, Naturwissenschaften 38, 159 (1951).
5. V.V. Vjadimirski, Zu. Eksp. Teor. Fiz. 39, 1062 (1960).
6. C.V. Heer, Rev. Sci. Instrum. 34, 532 (1963).
7. H.J. Metcalf, Nat. Bur. Stand. (U.S.) Spec. Publ. 653, 59 (1983).
8. W.H. Wing, Phys. Rev. Lett. 45, 631 (1980).
9. A. Ashkin, Phys. Rev. Lett. 40, 729 (1978).
10. A. Ashkin and J.P. Gordon, Opt. Lett. 4, 161 (1979).

3.9 Vibrationally Inelastic Collisions

National Science Foundation (Grant CHE79-02967-A04)

Thomas P. Scott, Neil Smith, Peter D. Magill, David E. Pritchard

In previous years we have exhaustively investigated Rotationally Inelastic (RI) collisions both theoretically and experimentally. We have shown the general applicability of scaling laws to these collisions and have illuminated general features of RI collisions using simple dynamical ideas.

We have now turned our attention to vibrationally–rotationally inelastic (VRI) processes for several major reasons. Firstly, it is now possible to study these collision processes with much greater detail than has been done previously. Secondly, no general theory exists for VRI collisions, inviting us to generalize the ideas which have developed for purely RI collisions to this more complicated situation. Finally, there is a need to reduce the thousands of vibrationally and rotationally level specific rate constants in order to model collision dynamics in many important regimes (e.g., planetary atmospheres, gas lasers, supersonic expansions).

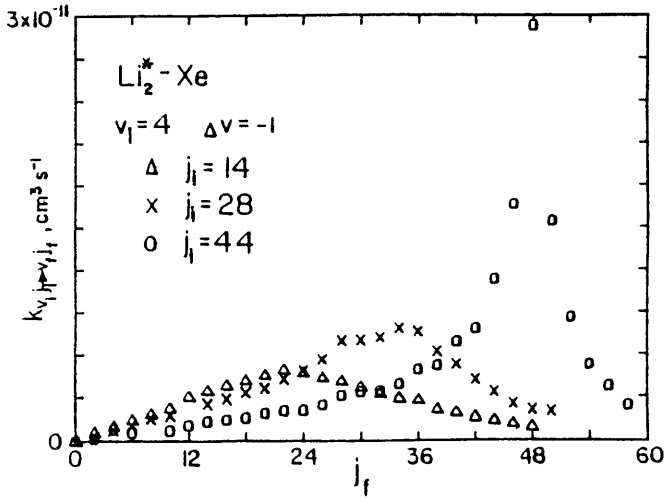

Figure 3-9:

Our initial measurements of VRI rate constants for $k_{v_i = 4, j_i \rightarrow v_f j_f}$ for the system Li_2^*–Xe (SSD83), has demonstrated a significant role of initial rotation quantum number, j_i, in determining the magnitude of $k_{v_i' j_i \rightarrow v_f j_f}$ and the specificity in the distribution of final rotational states for a given $\Delta v = v_{f v_i}$ (Fig. 3–9).

The peak of these distributions regardless of Δv is found to be given by the simple expression $(j_f)_{peak} = j_i - 4\Delta v$. This differs from the position of the peak given by energy resonance.

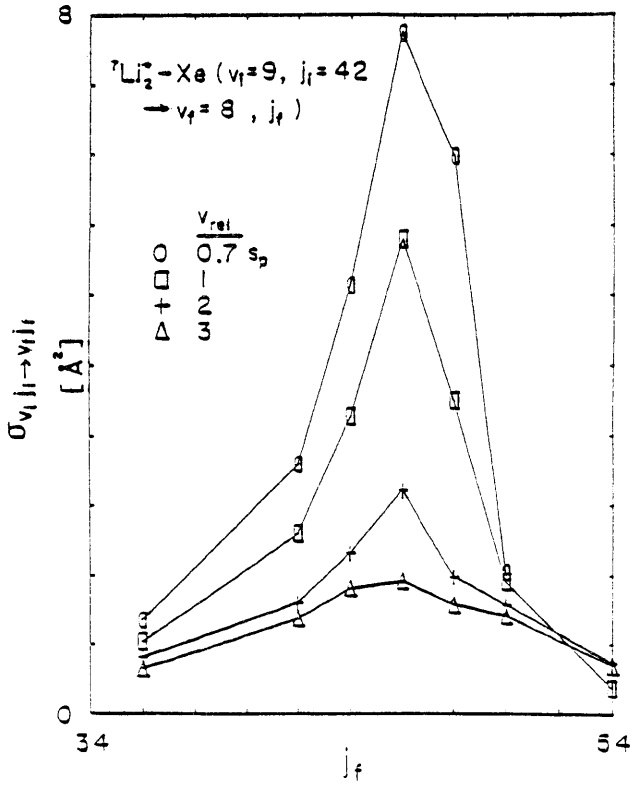

Figure 3-10:

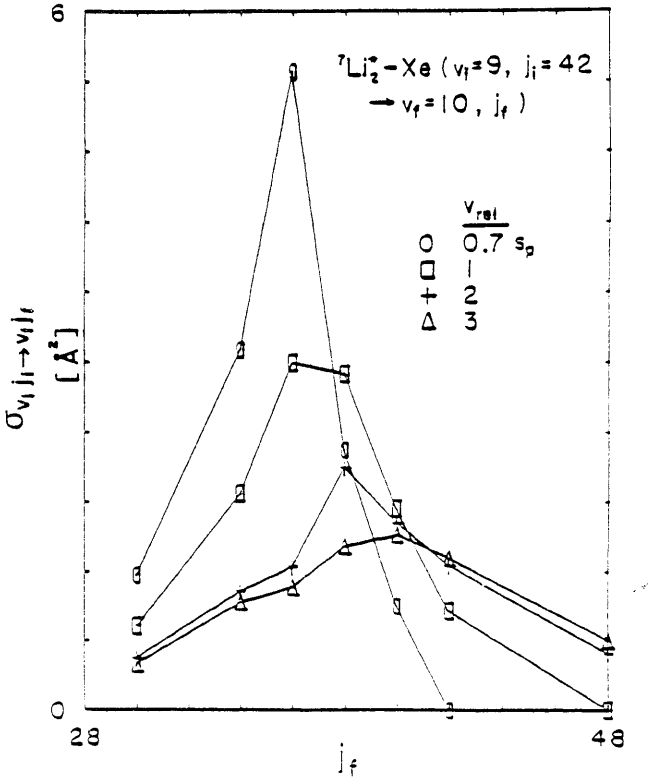

Figure 3-11:

Using our method of velocity selection by Doppler shift (VSDS) to measure the dependence of level to level specific cross sections on collisional velocity, we have measured the velocity dependence of these distributions for $Li_2^*(v_i = 9, j_i = 42 \to v_f, j_f) - Xe$ where $\Delta v = -1$ (Fig. 3–10) and $\Delta v = +1$ (Fig. 3–11). We find that the peak is reduced and the distribution is broadened as the collision velocity is increased. Further, while the peak of the $\Delta v = -1$ distribution is given by the $(j)_{fpeak} = j_i - 4\Delta v$ rule for all velocities, that for the $\Delta v = +1$ distribution moves toward higher j_f as the collision velocity is increased. For both values of Δv, the total VRI cross section (area under the peak) decreases monotonically with increasing collision velocity.

References

1. K.L. Saenger, N. Smith, S.L. Dexheimer, C. Engelke, and D.E. Pritchard, J. Chem. Phys. 79, 4076 (1983).